CHEMISTRY
A EUROPEAN JOURNAL

DOI: 10.1002/chem.200500351

What Anions Do Inside a Receptor's Cavity: A Trifurcate Anion Receptor Providing Both Electrostatic and Hydrogen-Bonding Interactions

Valeria Amendola,[a] Massimo Boiocchi,[b] Luigi Fabbrizzi,*[a] and Arianna Palchetti[a]

Abstract: The trifurcate receptor $\mathbf{1}^{3+}$ forms stable 1:1 complexes with halide and oxo anions in MeCN solution, as shown by spectrophotometric and ^{1}H NMR experiments, and selectively recognizes chloride ($\lg K_{ass} > 7$) in the presence of fluoride and bromide. The high stability reflects the receptor's ability to donate up to six hydrogen bonds (from three pyrrole N–H and three C–H fragments, polarized by the proximate positive charge) to the included anion. Addition of an excess of more basic anions (F^- and CH_3COO^-) induces stepwise deprotonation of the N–H groups, an event signalled by the appearance of a bright yellow color. Crystal and molecular structures are reported for the complex with NO_3^- and a capsule consisting of two interconnected trifurcate subunits, one of which includes an H-bound Br^- ion, while the other is doubly deprotonated and includes an H-bound water molecule. Finally, evidence is given for the formation in solution of an authentic complex of OH^-, in which H-bound hydroxide is included within the cavity of $\mathbf{1}^{3+}$.

Keywords: anions · hydrogen bonds · molecular recognition · receptors · supramolecular chemistry

Introduction

There is a current interest on the design of selective receptors for anions.[1,2] In general, a receptor is expected to provide a cavity in which to accommodate the envisaged guest. Moreover, the cavity should contain groups capable of interacting with the guest. Selectivity depends both on energy terms (related to the intensity of the receptor–substrate interaction) and on geometrical factors (size and shape matching between receptor and substrate). Anions are prone to interact through either electrostatic or H-bond interactions, and thus the receptor must contain either positively charged groups (ammonium,[3] alkylammonium,[4] guanidinium,[5] pyridinium,[6] imidazolium,[7] coordinatively unsaturated metal ions)[8] or neutral hydrogen-bond donor groups (amides,[9] sulfonamides,[10] ureas,[11] pyrroles).[12] A variety of charged and neutral anion receptors have been synthesized during the last two decades. Some of them have a closed polycyclic structure that forms a cage.[13] In others, arms containing the interacting groups are appended to a defined platform. For instance, amide derivatives of the tripodal tetramine tren have been used as trifurcate anion receptors.[14] A more rigid and preorganized scaffold used in the design of trifurcate anion receptors is the 1,3,5-substituted benzene subunit, the binding moieties of which in the 1,3,5-positions are directed to one face of the ring. For instance, on appending three aminoimidazoline arms to such a moiety, a receptor with triple positive electrical charge was obtained which is capable of recognizing the citrate anion in beverages.[15]

We designed the trifurcate receptor $\mathbf{1}^{3+}$, in which three

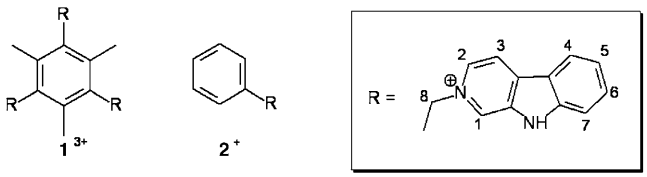

9*H*-β-carbolin-2-ium fragments are appended to the 1,3,5-benzene platform through methylene spacers. A recent study showed that the cationic receptor $\mathbf{2}^+$ containing a single 9*H*-β-carbolin-2-ium fragment undergoes rather strong interaction with most anions and, in particular, it is

[a] Dr. V. Amendola, Prof. L. Fabbrizzi, Dr. A. Palchetti
Dipartimento di Chimica Generale
Università di Pavia, viale Taramelli 12
27100 Pavia (Italy)
Fax: (+39) 0382-528544
E-mail: luigi.fabbrizzi@unipv.it

[b] Dr. M. Boiocchi
Centro Grandi Strumenti
Università di Pavia, via Bassi 21
27100 Pavia (Italy)

InterScience
© 2005 Wiley-VCH Verlag GmbH & Co. KGaA, Weinheim

able to transfer the N–H proton to the most basic anions (fluoride and acetate).[16] Moreover, a tricationic host based on the 1,3,5-benzene platform, containing three aminopyridinium groups and displaying a special affinity towards chloride, has been recently reported.[17] The trifurcate system described here is expected to exhibit stronger interactions with anions, in view of the more pronounced H-bond donor tendencies of the pyrrole N–H group with respect to the aniline N–H group.[18]

The interaction of trifurcate receptor $\mathbf{1}^{3+}$ with anions was investigated in MeCN solution by UV/Vis and ^{1}H NMR titration experiments. Parallel studies were carried out on the single-arm receptor $\mathbf{2}^{+}$ to verify 1) the effects associated with the geometrical features of the cavity, and 2) the cooperativity, if any, of electrostatic and hydrogen-bonding interactions. In particular, the binding tendencies of $\mathbf{2}^{+}$, previously investigated by us in DMSO, were completely reinvestigated in MeCN. Such an investigation is not a duplicate, as the polarity of the solvent affects substantially the establishment of hydrogen-bonding interactions and, in particular, deprotonation of the N–H group. Moreover, the crystal and molecular structure of the $\mathbf{1}^{3+}/NO_3^-$ inclusion complex is reported. Then, the serendipitous crystallization of a dimeric capsule formed by two interconnected receptors, in which one subunit includes a bromide ion and the other, in its doubly deprotonated form, incorporates a water molecule, allowed us to substantiate findings in solution and threw new light on the nature and mode of anion recognition based on H-bonding interactions.

Results and Discussion

Single-arm receptor $\mathbf{2}^{+}$: The interaction of receptor $\mathbf{2}^{+}$ with anions X^- was investigated by titrating a solution of **2**-PF_6 in MeCN with a standard solution of a tetraalkylammonium salt of X^-. In spectrophotometric titration experiments, the concentration of $\mathbf{2}^{+}$ varied over the range 10^{-4}–10^{-5} M. Figure 1 displays the family of absorption spectra obtained during titration with chloride. On Cl^- addition, the absorption band centered at 377 nm ($\varepsilon = 4.0\times10^3\,M^{-1}cm^{-1}$), assigned to the charge-transfer transition from pyrrole NH to the N^+ group of the adjacent pyridinium ring, is red-shifted, while definite isosbestic points formed at 282, 313, 328, and 387 nm. A titration profile, obtained by plotting the molar absorbance at 410 nm versus the number of added equivalents of chloride, is shown in the inset. Titration data are consistent with the formation of a 1:1 receptor:anion complex. Nonlinear least-squares treatment of the titration data gave a $\lg K$ value of 3.20 ± 0.01 for the equilibrium $\mathbf{2}^{+} + Cl^- \rightleftharpoons [\mathbf{2}\cdots Cl]$. The inset of Figure 1 also shows how the equilibrium concentrations $\mathbf{2}^{+}$ and $[\mathbf{2}\cdots Cl]$ vary on chloride addition. In particular, good superimposition of the profiles for absorbance and $[\mathbf{2}\cdots Cl]$ concentration is observed. Similar spectral behavior and formation of a 1:1 complex were observed on titration of $\mathbf{2}^{+}$ with Br^- and NO_3^-. Pertinent values of $\lg K$ are reported in Table 1. On titration with I^-, spectral modification was very moderate, even after addition of a large excess of anions, and a $\lg K$ value of less than 2 was estimated for formation of the 1:1 receptor:anion complex.

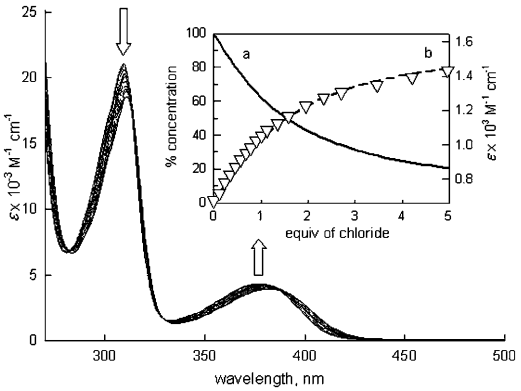

Figure 1. Spectrophotometric titration of a MeCN solution of **2**-PF_6 (6.2×10^{-4} M) with a standard MeCN solution of $[Bu_3BzN]Cl$. Inset: titration profile (molar absorbance ε at 410 nm versus number of equivalents of Cl^-). The distribution diagram (% concentration) is superimposed. Curve a (solid line) corresponds to the uncomplexed receptor $\mathbf{2}^{+}$, whereas curve b (dashed line) is relative to the chloride complex $[\mathbf{2}\cdots Cl]$.

Table 1. Constants of the complex formation equilibrium[a] in MeCN solution at 25 °C.

Anion	Receptor $\mathbf{2}^{+}$, $\log K$	Receptor $\mathbf{1}^{3+}$, $\log K$
Cl^-	3.20(1)	>7
Br^-	2.48(1)	6.65(2)
NO_3^-	2.58(1)	5.59(2)
I^-	<2	4.55(2)
Ac^-	$\log K_1 = 4.68(5)$	$\log K_1 = 4.37(5)$
	$\log K_2 = 1.63(9)$	$\log K_2 = 3.12(9)$
		$\log K_3 = 2.8(1)$
F^-	$\log K_1 = 6.19(5)$	$\log K_1 = 5.04(2)$
	$\log K_2 = 6.07(9)$	$\log K_2 = 2.79(5)$
		$\log K_3 = 4.02(6)$
OH^-	6.42(2)	$\log K_1 = 5.58$ (5)
		$\log K_2 = 3.92(9)$
		$\log K_3 = 5.7(1)$

[a] In parentheses: uncertainty in the last digit.

It was previously observed that, in DMSO solution, Cl^-, Br^-, and NO_3^- do not appreciably interact with $\mathbf{2}^{+}$, as judged from spectrophotometric titrations carried out in the same concentration range ($\lg K < 2$).[16] This reflects the higher solvating effect exerted by the more polar DMSO molecules (dielectric constant $\varepsilon = 47.24$ at 20 °C) compared to MeCN ($\varepsilon = 36.64$ at 20 °C). In particular, the energy contribution from the hydrogen-bond interaction does not compensate for the unfavorable term related to desolvation of the anion. Thus, the use of the less polar solvent MeCN instead of DMSO ensures formation and allows characterization of complexes of a greater number of anions.

Figure 2 shows selected ^{1}H NMR spectra recorded over the course of the titration with Cl^- of a 10^{-2} M solution of **2**-PF_6 in CD_3CN. The NH signal could not be observed, even

 © 2005 Wiley-VCH Verlag GmbH & Co. KGaA, Weinheim

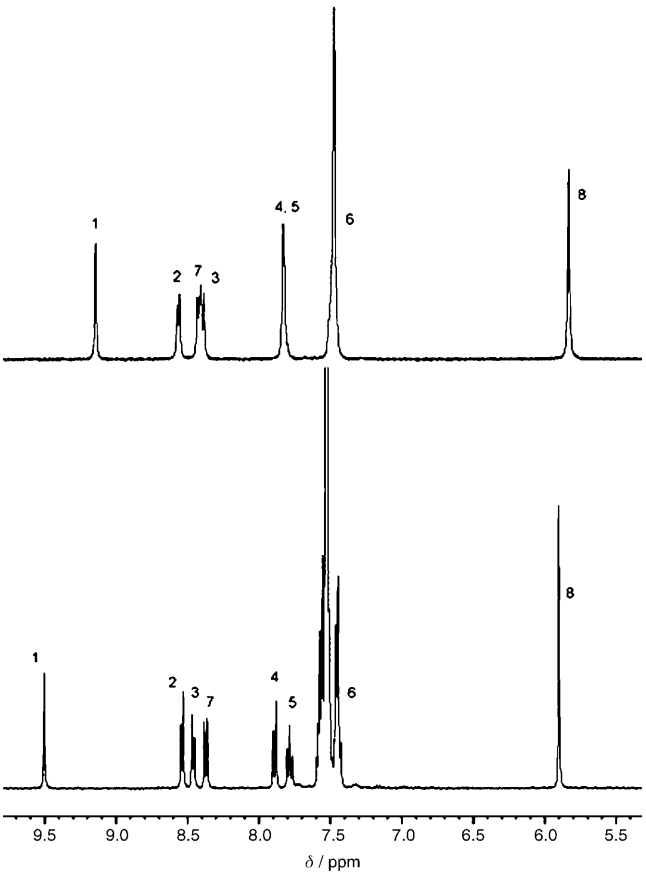

Figure 2. ^{1}H NMR titration of a CD_3CN solution of **2**-PF_6 (10^{-2} M) with a standard CD_3CN solution of $[Bu_3BzN]Cl$. The spectra were recorded on a solution of **2**-PF_6 (top) and after addition of an excess of chloride (bottom).

C–H bonds close to the interaction site. In fact, in the case of the CH(1) proton, the electrostatic effect dominates and a progressive downfield shift is observed, which stops after addition of excess Cl^-. On the other hand, the CH protons of the phenyl ring fused to the pyrrole subunit do not feel the anion-induced electrostatic effect and are affected only by the through-bond contribution, which induces a slight upfield shift. Thus, spectroscopic data suggest the establishment of hydrogen-bond interactions between Cl^- and 1) the pyrrole NH group, and 2) the CH(1) fragment.

The more basic anions F^- and CH_3COO^- exhibited different behavior. Figure 3 shows the family of UV/Vis spectra

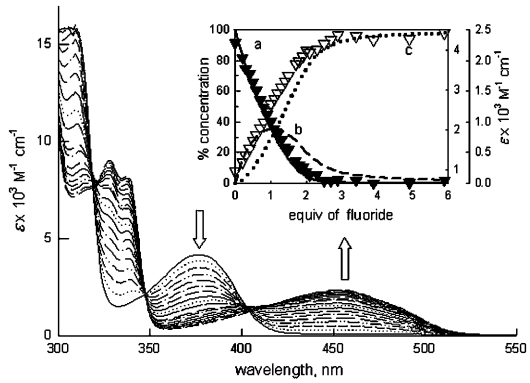

Figure 3. Spectrophotometric titration of a MeCN solution of **2**-PF_6 (1.1×10^{-4} M) with a standard MeCN solution of $[Bu_4N]F$. Inset: titration profile relative to the titration of a 10^{-5} M solution of [4]PF_6 with fluoride (molar absorbance ε at 380 (filled symbols) and 454 nm (open symbols) versus the number of equivalents of F^-). The distribution diagram of the species (% concentration) versus number of equivalents of F^- is superimposed: a) LH^+, solid line; b) $[LH\cdots F]^-$, dashed line; c) L, dotted line.

prior to addition of chloride. This may be due to fast proton exchange with water present in solution. Anhydrous CD_3CN was used and care was taken to avoid contamination with water in preparation of the solution and during titration, but it appears that trace water concentrations in the solution are high enough to ensure fast proton exchange and disappearance of the N–H signal. On the other hand, in the case of the anion complexes of the trifurcate receptor $\mathbf{1}^{3+}$, a sharp NH signal can be observed (vide infra), probably due to the cone arrangement of the receptor, which prevents access of water to the cavity. The most evident spectral modification was the downfield shift of H(1) from $\delta=9.15$ to 9.50 ppm ($\Delta\delta=+0.35$) on addition of excess Cl^-. The anion–receptor interaction is expected to generate two distinct effects: 1) an increase in the electron density on the receptor framework (in particular, on the phenyl rings) by through-bond propagation, which causes a shielding effect and should promote an upfield shift of the C–H signals; and 2) polarization of the C–H bonds, induced by a through-space effect, of electrostatic nature; in particular, the partial positive charge created onto the proton induces a deshielding effect and consequent downfield shift. The latter effect is expected to disappear at larger distances and should therefore affect only the

recorded over the course of the titration of a solution of $[\mathbf{2}]^+$ in MeCN (1.1×10^{-4} M) with tetrabutylammonium fluoride. On addition of fluoride, the band at 380 nm decreased, while a new band formed and developed at 454 nm. Furthermore, addition of the anion induced a change in the color of the solution from pale to bright yellow. The titration curves of the two bands (inset) reached a limiting value after the addition of two equivalents of F^-. Nonlinear least-squares treatment of the titration data indicated the occurrence of two consecutive equilibria, with $\lg K_1=6.19\pm0.04$ and $\lg K_2=6.07\pm0.09$. It is suggested that the first equilibrium leads to the formation of a genuine 1:1 hydrogen-bond complex, whereas the second involves deprotonation of the NH group with formation of $[HF_2]^-$, as described by Equations (1) and (2) (where the receptor $\mathbf{2}^+$ is indicated as LH^+ and F^- as X^-).

$$LH^+ + X^- \rightleftharpoons [LH\cdots X]^- \quad (1)$$

$$[LH\cdots X] + X^- \rightleftharpoons L + [HX_2]^- \quad (2)$$

The nature of the two consecutive equilibria (1) and (2) was substantiated by ^{1}H NMR titration experiments.

 © 2005 Wiley-VCH Verlag GmbH & Co. KGaA, Weinheim

Figure 4 shows the spectra obtained on titration of a solution of **2**-PF_6 in CD_3CN with a standard solution of Bu_4NF in CD_3CN. During addition of the first equivalent, a downfield shift of CH(1) is observed ($\Delta\delta = +0.11$), which is ascribed to the polarization effect exerted by the proximate F^- ion, hydrogen-bonded to the pyrrole NH fragment (Figure 4a–c). On further addition of fluoride, the CH(1) signal undergoes significant upfield shift and reaches the limiting value of $\delta = 8.90$ ppm ($\Delta\delta = -0.32$) after addition of 2.5 equivalents (Figure 4d,e). Such behavior is consistent with deprotonation of the NH group. In the resulting zwitterion, π-delocalization of the negative electrical charge over the entire molecular framework should take place, as illustrated by the resonance forms in Scheme 1. Such a through-bond effect increases nuclear shielding and induces a general upfield shift of CH signals. Upfield shift of CH protons has been observed in a sulfonamide-based receptor, the N–H fragment of which had been deprotonated by an F^- anion.[16]

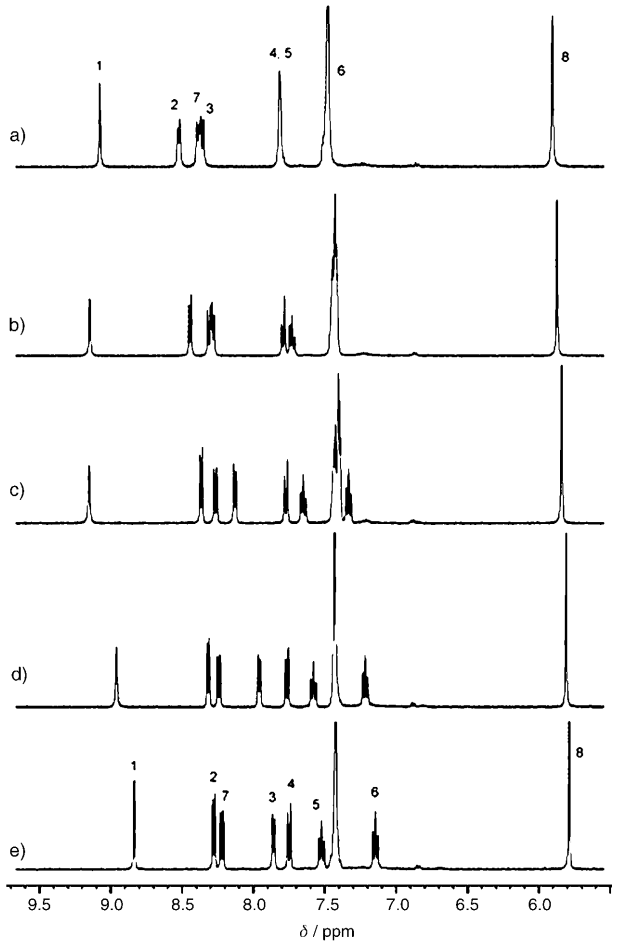

Figure 4. ^1H NMR titration of a CD_3CN solution of **2**-PF_6 (10^{-2} M) with a standard CD_3CN solution of $[Bu_4N]F$. The reported spectra were registered after the addition of 0 (a), 0.25 (b), 0.75 (c), 1.50 (d), and 2.50 equivalents (e) of fluoride.

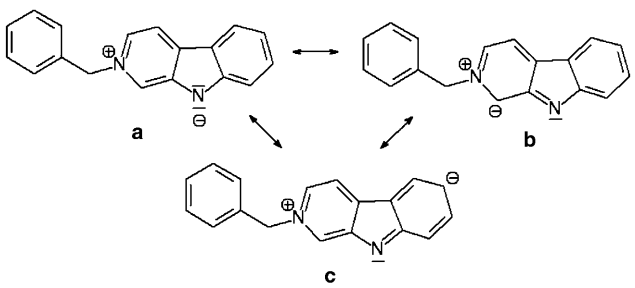

Scheme 1. Resonance representation of the zwitterion resulting from deprotonation of the NH fragment of $\mathbf{2}^+$. Only some limiting formulas are shown.

Fluoride establishes by far the strongest hydrogen-bonding interaction among halide anions, as indicated by the highest value of $\lg K_1$. In spite of this, the [LH···F] complex is not stable with respect to further fluoride addition. In the presence of excess F^-, the N–H group is deprotonated or, more precisely, the [LH···F] complex releases an HF molecule, which interacts with fluoride to give the $[HF_2]^-$ anion. This is due to the very high stability of $[HF_2]^-$, the hydrogen-bond complex for which the highest hydrogen bond energy in the gas phase has been calculated (39 kcal mol^{-1}).[18] Fluoride-induced deprotonation of the NH group of 3,4-dichloro-2,5-diamidopyrroles has been previously detected by means of ^1H NMR titration experiments in CH_2Cl_2 solution.[19] In particular, NH acidity was enhanced by electron-withdrawing substituents in the 3- and 4-positions. In the present case, the acidic properties of the pyrrole fragment are drastically increased by the presence of a proximate positively charged group.

Formation of the zwitterion L accounts for the spectrophotometric behavior. On NH deprotonation, the intensity of the dipole responsible for the charge-transfer transition is drastically enhanced and thus induces a large red shift of the absorption band (from 380 to 454 nm). Therefore, the appearance of a charge-transfer band at long wavelength should be taken as a distinctive indication of the occurrence of NH deprotonation. However, it may be surprising that such a band pertinent to LH starts to develop on initial addition of F^-, and its absorbance increases up to the addition of two equivalents. The apparent paradox can be explained by considering that K_2 is especially high and, in particular, it is equal, within the standard deviation, to K_1. For this reason, the zwitterion L forms almost simultaneously with the hydrogen-bonded complex [LH···F] (see the distribution diagram in the inset of Figure 3). Notably, the profiles of the absorbance of the bands at 380 (filled symbols) and 454 nm (open symbols) superimpose well on the concentration curves of LH^+ (a) and L (c), respectively (see inset to Figure 3).

Figure 5 shows the absorption spectra recorded in the course of the titration of a solution of **2**-PF_6 in MeCN (2.1×10^{-4} M) with a standard solution of $[Bu_4N]CH_3COO$ in MeCN. The spectra are very similar to those obtained on titration with fluoride. In particular, on addition of acetate,

 © 2005 Wiley-VCH Verlag GmbH & Co. KGaA, Weinheim

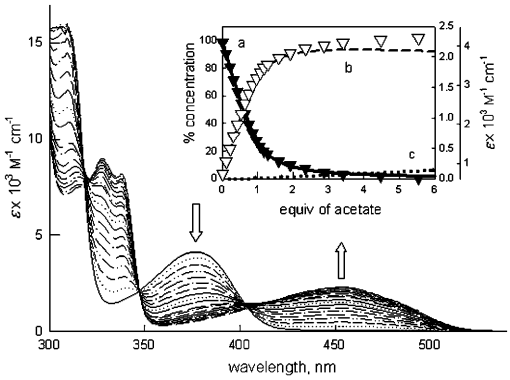

Figure 5. Spectrophotometric titration of a MeCN solution of **2**-PF_6 (2.1×10^{-4} M) with a standard MeCN solution of $[Bu_4N]CH_3COO$. Inset: titration profile relative to the titration of a 2.1×10^{-4} M solution of **2**-PF_6 with acetate (molar absorbance ε at 380 nm (filled symbols) and at 454 nm (open symbols) versus number of equivalents of acetate). The distribution diagram of the species (% concentration) versus the number of equivalents of anion is superimposed: a) LH^+, solid line; b) $[LH\cdots Ac]^-$, dashed line; c) L, dotted line.

the charge-transfer band of $\mathbf{2}^+$ at 380 nm disappears, while a band forms and develops at 454 nm (indicative of NH deprotonation). The absorbance versus equivalents of CH_3COO^- plots (for bands at 380 and 454 nm, see inset) show a rather steep profile until 1 equiv of titrant has been added, then become smooth, and reach a plateau for excess acetate. Best fits of the titration data were obtained on the basis of two stepwise equilibria with $\lg K_1 = 4.68\pm0.04$ and $\lg K_2 = 1.63\pm0.09$. Also in this case, decisive information on the nature of the species at equilibrium came from ^{1}H NMR titration experiments. Pertinent spectra are shown in Figure 6.

On addition of the first equivalent of acetate, a distinct downfield shift of the CH(1) proton is observed ($\Delta\delta = +0.41$ after addition of one equivalent of acetate, compared to $\Delta\delta = +0.11$ after the addition of one equivalent of fluoride). At the same time, the CH protons of the phenyl ring fused to the pyrrole subunit undergo substantial upfield shifts. Upfield shift and development of the absorption band at 454 nm indicate the occurrence of NH deprotonation. On the other hand, the pronounced downfield shift of the CH(1) proton provides evidence for hydrogen-bonding interaction. Thus, it is suggested that proton transfer takes place from NH to CH_3COO^- to form CH_3COOH. On the other hand, the C=O oxygen atom of acetic acid establishes an H-bonding interaction with the strongly polarized C–H(1) fragment. In other words, in the $\mathbf{2}^+/CH_3COO^-$ complex which forms, intracomplex proton transfer takes place. Then, on addition of further acetate, all protons undergo upfield shifts, including C–H(1). This is consistent with the full release of CH_3COOH from the receptor to form the $[CH_3COOH\cdots CH_3COO]^-$ H-bonded self-complex. It has been pointed out that the most stable H-bonded complex an anion can form is that with its conjugate acid.[20] However, the base/conjugate acid complex of acetate $[CH_3COOH\cdots CH_3COO]^-$ is considerably less stable than

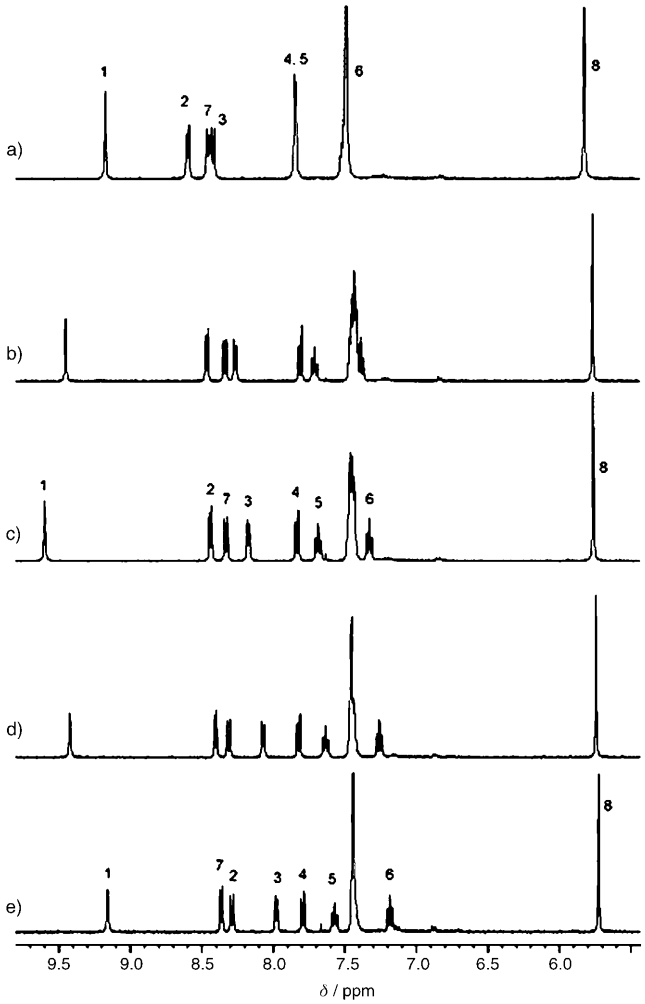

Figure 6. ^{1}H NMR titration of a CD_3CN solution of **2**-PF_6 (10^{-2} M) with a standard CD_3CN solution of $[Bu_4N]CH_3COO$. The spectra were recorded after addition of 0 (a), 0.50 (b), 1.0 (c), 2.0 (d), and 5.0 equivalents (e) of acetate.

$[HF_2]^-$, and excess equivalents of CH_3COO^- are required to achieve significant formation of the zwitterion L (note that the distribution diagram shown in the inset of Figure 5 refers to the spectrophotometric titration experiment, in which the analytical concentration of $\mathbf{2}^+$ was 2.1×10^{-4} M; in the ^{1}H NMR titration experiment, the analytical concentration of $\mathbf{2}^+$ was much higher, 1×10^{-2} M, which made the concentration of the zwitterion L distinctly higher in presence of the same excess of acetate). In any case, the complex $[L\cdots CH_3COOH]$ formed in the first stepwise equilibrium shows the same spectrum as the distinct zwitterion L obtained on titration with fluoride, and this indicates that the H-bonding interaction with CH_3COOH does not affect the pertinent charge-transfer transition.

Changes in solvent polarity have a dramatic effect on the interaction of $\mathbf{2}^+$ with the more basic anions F^- and CH_3COO^-. In DMSO solution, no intermediate formation of the $[LH\cdots X]$ hydrogen-bonded complex was observed, but NH deprotonation and release of HX occurred on addi-

 © 2005 Wiley-VCH Verlag GmbH & Co. KGaA, Weinheim

tion of the first equivalent of X^-. The $\lg K_N$ values for the neutralization equilibrium $[LH]^+ + X^- \rightleftharpoons [L] + HX$ were 5.10 ± 0.05 for CH_3COO^- and 4.77 ± 0.02 for F^-. One-step deprotonation of $[LH]^+$ may reflect stabilization of the [L] zwitterion by DMSO. Such an effect is not observed with the less polar MeCN, in which deprotonation is associated with formation of the $[HX_2]^-$ self-complex. In this connection, it is useful to consider the overall neutralization equilibrium [Eq. (3)].

$$[LH]^+ + 2X^- \rightleftharpoons [L] + [HX_2]^- \quad (3)$$

Note that the neutralization equilibrium [Eq. (3)] results from the sum of Equations (1) and (2), from which the following equation derives: $\beta_N = K_1 \times K_2 = 6.3$ for acetate and 12.3 for fluoride. The β_N value corresponds to the product of the intrinsic acidity constant of $[LH]^+$ and the formation constant of the $[HX_2]^-$ self-complex: $\beta_N = K_A(LH) \times \beta(HX_2^-)$, where $\beta(HX_2^-) = [HX_2^-]/([H^+] \times [X^-]^2)$. Thus, the highly favored deprotonation of $[LH]^+$ in the presence of F^- in MeCN solution reflects the unique stability of the $[HF_2]^-$ self-complex. In fact, the much less stable $[CH_3COOH \cdots CH_3COO]^-$ self-complex forms in detectable amounts only on addition of a large excess of acetate (see the green concentration profile in the inset to Figure 5).

At this stage, it seemed convenient to look at the interaction of $\mathbf{2}^+$ with the strongest basic anion: OH^-. Figure 7

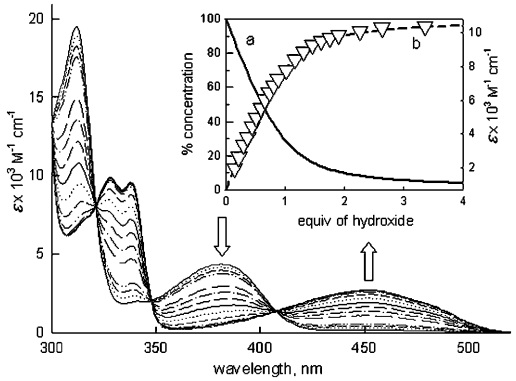

Figure 7. Spectrophotometric titration of a MeCN solution of **2**-PF_6 (5.2×10^{-4} M) with a standard MeCN solution of $[Bu_4N]OH$. Inset: titration profile relative to the titration with $[Bu_4N]OH$ of a 5×10^{-6} M solution of **2**-PF_6 (for this experiment, a path length of 10 cm was required); molar absorbance ε at 335 nm versus number of equivalents of hydroxide. The distribution diagram (% concentration) is also reported: a) LH^+, solid line; b) zwitterion L, dashed line.

shows the UV/Vis spectra obtained on titration of a solution of **2**-PF_6 in MeCN (5.2×10^{-4} M) with a solution of $[Bu_4N]OH$ in MeCN. On addition of hydroxide, the band at 454 nm develops and reaches its limiting value after the addition of one equivalent; simultaneous development of a yellow color is observed. ^{1}H NMR titration experiments showed general upfield shift of all CH protons following initial addition of titrant, which ceased after the addition of one equivalent of OH^-. This indicates the occurrence of single-step deprotonation of the pyrrole subunit with formation of the zwitterion L ($\lg K = 6.42 \pm 0.02$).

In summary, halides and nitrate form 1:1 H-bonded complexes with the charged receptor $\mathbf{2}^+$, whose stability decreases along the series: $F^- > Cl^- > NO_3^- > Br^- > I^-$, which reflects anion basicity in MeCN. Acetate gives a special hydrogen-bonded complex in which the NH proton has been intramolecularly transferred to CH_3COO^-, and the C=O fragment of the anion is hydrogen-bonded to CH(1) and acts as a pivot. Fluoride and acetate give the most stable 1:1 complexes, but they are not stable with respect to further anion addition, due to the formation of the $[HX_2]^-$ self-complex. Only the strongly basic OH^- anion is able to induce deprotonation of $\mathbf{2}^+$ in a single step.

Trifurcate receptor $\mathbf{1}^{3+}$: Figure 8 shows the family of spectra recorded in the course of the spectrophotometric titration of

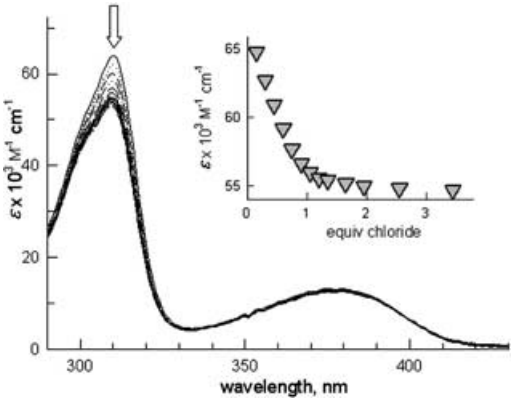

Figure 8. Spectrophotometric titration of an MeCN solution of **1**-$(PF_6)_3$ (5.0×10^{-6} M) with a standard MeCN solution of $[Bu_3BzN]Cl$. Inset: titration profile (molar absorbance ε at 310 nm versus the number of equivalents of Cl^-).

a solution of **1**-$(PF_6)_3$ in MeCN (5.0×10^{-6}) with $[Bu_3Bz]Cl$. On chloride addition, moderate, yet distinct modifications of the spectral pattern were observed. The inset displays the plot of the molar absorbance at 310 nm versus equivalents of chloride: such a titration profile indicates the formation of a 1:1 complex. The titration profile showed a steep curvature (even under dilute conditions, e.g., 5×10^{-6} M), which should correspond to an especially high equilibrium constant. In particular, the p parameter (p = [concentration of complex]/[maximum possible concentration of complex]) was in any case higher than 0.8, a condition which does not allow the determination of a reliable equilibrium constant. Thus, we can only state that $\lg K$ is greater than 7.

Figure 9 shows the ^{1}H NMR spectra obtained during the titration with chloride of a solution of **1**-$(PF_6)_3$ in CD_3CN (1.1×10^{-3} M). Interestingly, the N–H signal is now clearly observed, and this may be due to the fact that, in the trifurcate receptor, the pyrrole subunits are not exposed to the solvent, but stay inside a cavity, access to which is controlled

 © 2005 Wiley-VCH Verlag GmbH & Co. KGaA, Weinheim

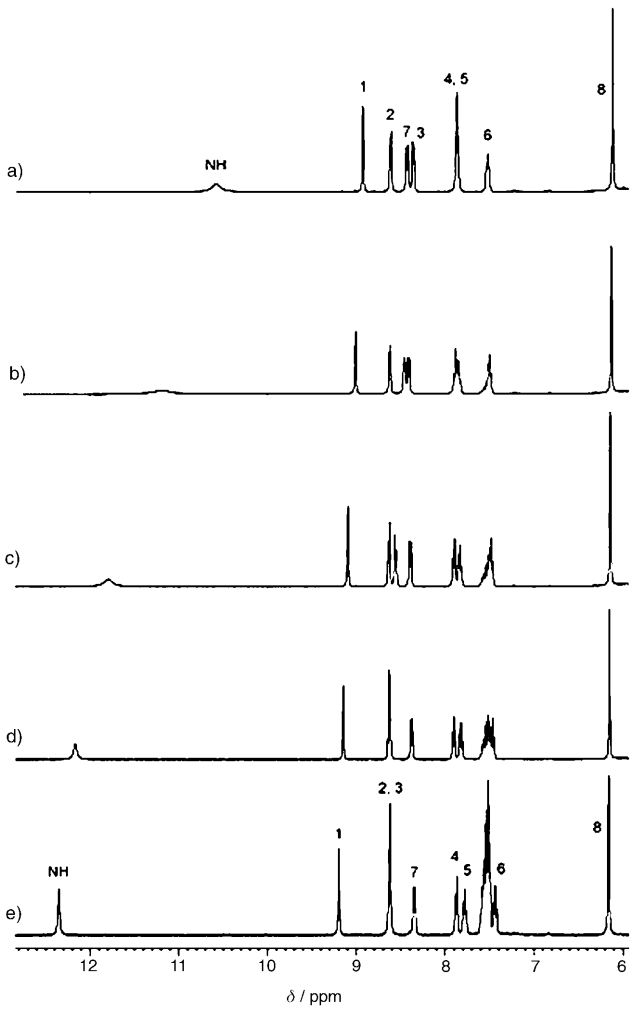

Figure 9. ^{1}H NMR titration of a CD_3CN solution of **1**-$(PF_6)_3$ (1.1×10^{-3} M) with a standard CD_3CN solution of $[Bu_3BzN]Cl$. The spectra were recorded after the addition of 0 (a), 0.35 (b), 0.70 (c), 1.00 (d), and 1.90 equivalents (e) of chloride.

by the aromatic rings fused to the pyrrole moieties. This may hinder the access of trace water molecules to the cavity and thus reduce proton exchange with the NH groups. Moreover, addition of chloride shifts the NH and CH(1) signals downfield, and this suggests formation of a stable H-bonded complex in which the anion is bound to all of the N–H and C–H(1) donors. In the complex, the presence of the anion in the cavity of the receptor completely prevents exchange of the NH proton with the solvent; this would explain the fact that the N–H signal becomes sharper as the complex forms (Figure 9d). Occurrence of full chloride coordination is also suggested by the very high value of the association constant, which is more than four orders of magnitude larger than that of the corresponding complex with single-arm donor $\mathbf{2}^+$. To our knowledge, this is the largest association constant observed for an hydrogen-bonded complex of chloride with a synthetic receptor, in whatever medium.

Similar behavior was observed for bromide, iodide, and nitrate: moderate modification of the UV/Vis spectra and downfield shift of NH and CH(1) signals. Corresponding values of the association constants for the 1:1 hydrogen-bonded complexes are reported in Table 1; note that they are at least 10^3 times higher than those observed for reference system $\mathbf{2}^+$ and decrease along the "regular series" $Cl^- > NO_3^- > Br^- > I^-$. Acetate and fluoride display a much more intricate behavior. Figure 10 shows the UV/Vis spectra recorded in the course of the titration of **1**-$(PF_6)_3$ with CH_3COO^-.

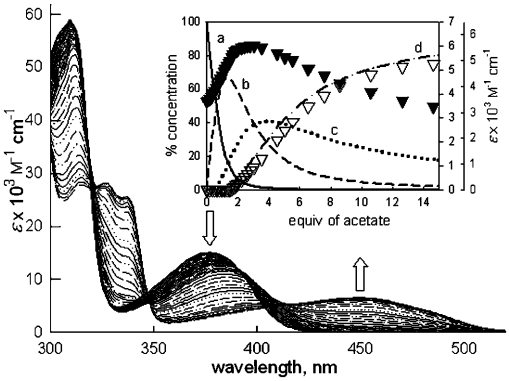

Figure 10. Spectrophotometric titration of a MeCN solution of **1**-$(PF_6)_3$ (1.0×10^{-4} M) with a standard MeCN solution of $[Bu_4N]CH_3COO$. Inset: titration profile (molar absorbance at 403 nm (filled triangles, right vertical axis) and at 450 nm (open triangles, right offset vertical axis) versus the number of equivalents of acetate); the distribution diagram (% concentration) of the species versus the number of equivalents of anion is superimposed: a) LH_3^{3+}, solid line; b) $[LH_3\cdots X]^{2+}$, dashed line; c) $[LH_3\cdots 2X]^{+}$, dotted line; d) $[L\cdots 3HX]$, $X^- = CH_3COO^-$, dash-dot line.

On anion addition, the band at 380 nm shifts to lower energy (389 nm), while its intensity decreases. After addition of 2 equiv, the color turns to yellow, the band at 389 nm starts to decrease, and a new band develops at 450 nm. Corresponding titration profiles (molar absorbance at the given wavelength vs equiv of CH_3COO^-) are shown in the inset to Figure 10. Studies on the single-arm reference system $\mathbf{2}^+$ showed that moderate shift of the band at 380 nm is suggestive of hydrogen-bonding interaction, while appearance of the band at 450 nm indicates NH deprotonation. On these bases, the occurrence of the following stepwise equilibria is tentatively proposed [Eqs. (4)–(6); $LH_3^{3+} = \mathbf{1}^{3+}$, $X^- = CH_3COO^-$].

$$LH_3^{3+} + X^- \rightleftharpoons [LH_3\cdots X]^{2+} \quad (4)$$

$$[LH_3\cdots X]^{2+} + X^- \rightleftharpoons [LH_3\cdots 2X]^{+} \quad (5)$$

$$[LH_3\cdots 2X]^{+} + X^- \rightleftharpoons [L\cdots 3HX] \quad (6)$$

Nonlinear least-squares fitting of the spectrophotometric titration data gave the following stepwise equilibrium constants: $\lg K_1 = 4.37\pm0.05$, $\lg K_2 = 3.12\pm0.09$, $\lg K_3 = 2.8\pm0.1$. Distribution curves of the species present at the equilibrium

 © 2005 Wiley-VCH Verlag GmbH & Co. KGaA, Weinheim

are shown in the inset to Figure 10; each curve fits quite well the profile of the absorbance of significant UV/Vis band. The presence of three positive charges in in $\mathbf{1}^{3+}$ seems to make hydrogen-bonding/electrostatic interactions with anions more favorable than deprotonation. In fact, the first two equivalents of CH_3COO^- enter the receptor's cavity to give the species $[LH_3\cdots X]^{2+}$ and $[LH_3\cdots 2X]^{+}$. The total absence of the band at 450 nm in these first two steps demonstrates that complexation does not involve deprotonation of the NH groups. Due to its Y-shape, the acetate ion does not fit well the C_{3v}-symmetric cavity of the host. The distinctly lower value of $\lg K_2$ with respect to $\lg K_1$ may reflect the endothermic rearrangement that the receptor must undergo when accomodating the second guest. After the addition of the first 2 equiv of acetate, the positive charge on the receptor is strongly reduced; furthermore, in the receptor's cavity, there is no room for accommodation of a third CH_3COO^- ion. Thus, on addition of the third equivalent and more, deprotonation occurs, with the development of the charge-transfer band at 450 nm and appearance of the yellow color.

These hypotheses are supported by the ^{1}H NMR titration experiment (see Figure 11). On addition of the first two equivalents of CH_3COO^-, the CH(1) protons shift slightly upfield due to moderate shielding (spectra a–c). This suggests that the CH(1) proton is not directly involved in H-bonding interaction, as observed in the case of single-arm receptor $\mathbf{2}^{+}$. Possibly, in the first step, the CH_3COO^- ion bridges two NH groups from two different arms. The N–H signal disappears after initial addition of the $[Bu_4N]CH_3COO$ solution; this may reflect a steric rearrangement of the trifurcate receptor, which opens the cavity to trace water molecules from the bulk and thus favors proton exchange. After addition of two equivalents, significant changes are observed (spectra d and e). In particular, the CH(1) signal is shifted downfield, whereas all other protons undergo upfield shifts. Similar behavior was observed in the interaction of CH_3COO^- with $\mathbf{2}^{+}$ and is indicative of the occurrence of an intramolecular proton transfer from pyrrole NH to an oxygen atom of acetate. Thus, it is suggested that the [L···3HX] complex is formed, in which each CH_3COOH molecule is hydrogen-bonded to one arm of the fully deprotonated receptor. The CH_3COOH molecule accepts a hydrogen bond from CH(1) and donates a hydrogen bond to the deprotonated nitrogen atom. At this point, one could ask how the trifurcate receptor could accommodate three acetic acid molecules inside its cavity. However, one should consider that each arm can rotate around the $-CH_2-$ group in the 8-position to expose its pyrrole subunit to the outside. Such an arrangement would allow easy and uncrowded interaction with the three binding sites. Finally, on addition of a large excess of anion, all protons undergo upfield shift, including CH(1) (spectrum f). This is consistent with full release of CH_3COOH from the receptor to form the $[CH_3COOH\cdots CH_3COO]^-$ hydrogen-bonded complex. Note that the three stepwise equilibria eventually leading to the zwitterion L were not considered in the calculation of the constants from spectrophotometric titration. They should be characterized by $\lg K$ values less than 2 and are not relevant at 10^{-4} M concentration.

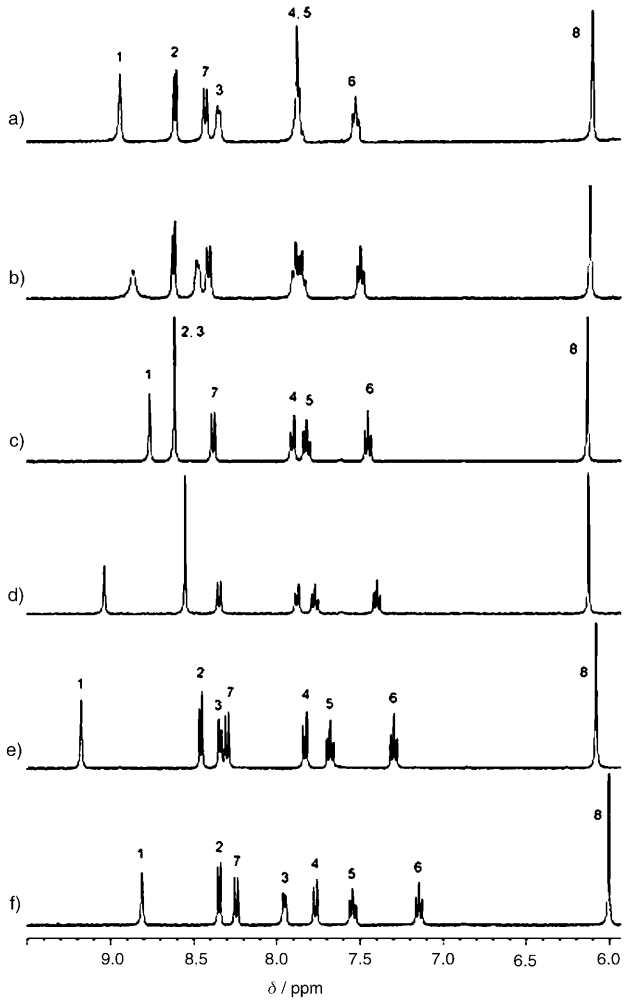

Figure 11. ^{1}H NMR titration of a CD_3CN solution of $\mathbf{1}$-$(PF_6)_3$ (1.0×10^{-3} M) with a standard CD_3CN solution of $[Bu_4N]CH_3COO$. The spectra were recorded after the addition of 0 (a), 0.80 (b), 2.0 (c), 2.8 (d), 5.0 (e), 12.5 equivalents (f) of acetate.

The behavior of fluoride is similar in part to that of acetate. Figure 12 shows the family of UV/Vis spectra obtained during the titration. Also in the present case, the band pertinent to the deprotonated receptor ($\lambda_{max}=450$ nm) begins to develop on addition of the third equivalent of anion. Spectral data are best fitted on the basis of three stepwise equilibria, the $\lg K$ values of which are reported in Table 1. The ^{1}H NMR spectra are not as well defined as those observed on acetate titration. General upfield shift of proton signals is observed following addition of the third equivalent of fluoride. This suggests that the third equilibrium should involve the disaggregation of the H-bonded complex $[LH_3\cdots 2X]^+$, with release of three molecules of HF and formation of the zwitterion [Eq. (7)].

$$[LH_3\cdots 2F]^+ + F^- \rightleftharpoons [L] + 3\,HF \qquad (7)$$

 © 2005 Wiley-VCH Verlag GmbH & Co. KGaA, Weinheim

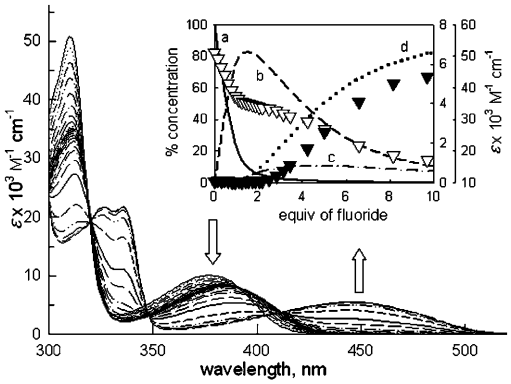

Figure 12. Spectrophotometric titration of a MeCN solution of **1**-$(PF_6)_3$ (1.0×10^{-4} M) with a standard MeCN solution of $[Bu_4N]F$. Inset: titration profile (molar absorbance ε at 310 nm (filled triangles, right vertical axis) and at 450 nm (open triangles, right offset vertical axis)). The distribution diagram of the species (% concentration) versus the number of equivalents of anion is superimposed: a) LH_3^{3+}, solid line; b) $[LH_3\cdots X]^{2+}$, dashed line; c) $[LH_3\cdots 2X]^{+}$, dash-dot line; d) L, dotted line.

Equilibrium (7) is progressively displaced to the right on addition of excess fluoride and formation of $[HF_2]^-$. Interestingly, the association constant for the 1:1 complex of fluoride with $\mathbf{1}^{3+}$ is much lower than those of the corresponding complexes of chloride and bromide, that is, the stability sequence typically observed for halide complexes with hydrogen-bond-donating receptors is inverted. This may be due to the fact that Cl^- and Br^- ions are large enough to interact with the NH and CH(1) fragments of the three arms of the trifurcate receptor to give a six-coordinate complex. On the other hand, the F^- ion is too small to encompass all the hydrogen-bond-donor groups of $\mathbf{1}^{3+}$ and can only profit from interaction with a single arm. Thus, receptor $\mathbf{1}^{3+}$ is able to recognize chloride in presence of fluoride, a quite rare circumstance in anion chemistry.

Finally, titration experiments were carried out with $[Bu_4N]OH$ as a titrant. Figure 13 shows the results of the spectrophotometric titration. Surprisingly, no significant modifications were observed in the UV/Vis spectrum during addition of the first equivalent of OH^-. Then, on addition of the second and third equivalents of hydroxide, the band at 450 nm developed and reached a limiting value (see the titration profile in the inset of Figure 13).

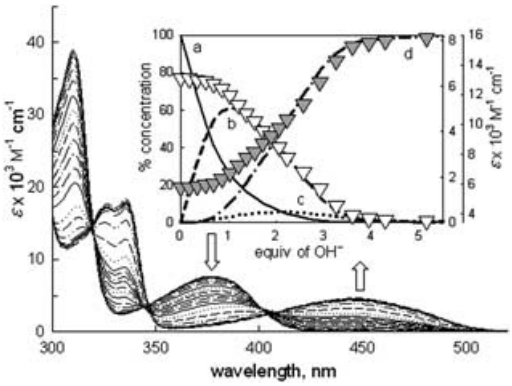

Figure 13. Spectrophotometric titration of a MeCN solution of **1**-$(PF_6)_3$ (1.0×10^{-3} M) with a standard MeCN solution of $[Bu_4N]OH$. Inset: titration profile (molar absorbance at 310 nm (filled triangles, right vertical axis) and 450 nm (open triangles, right offset vertical axis)). The distribution diagram of the species (% concentration) versus the number of equivalents of anion is superimposed: a) LH_3^{3+}, solid line; b) $[LH_3\cdots OH]^{2+}$, dashed line; c) LH^+, dotted line; d) L, dash-dot line.

In the ^{1}H NMR titration experiment (see spectra in Figure 14), the CH(1) signal underwent downfield shift from

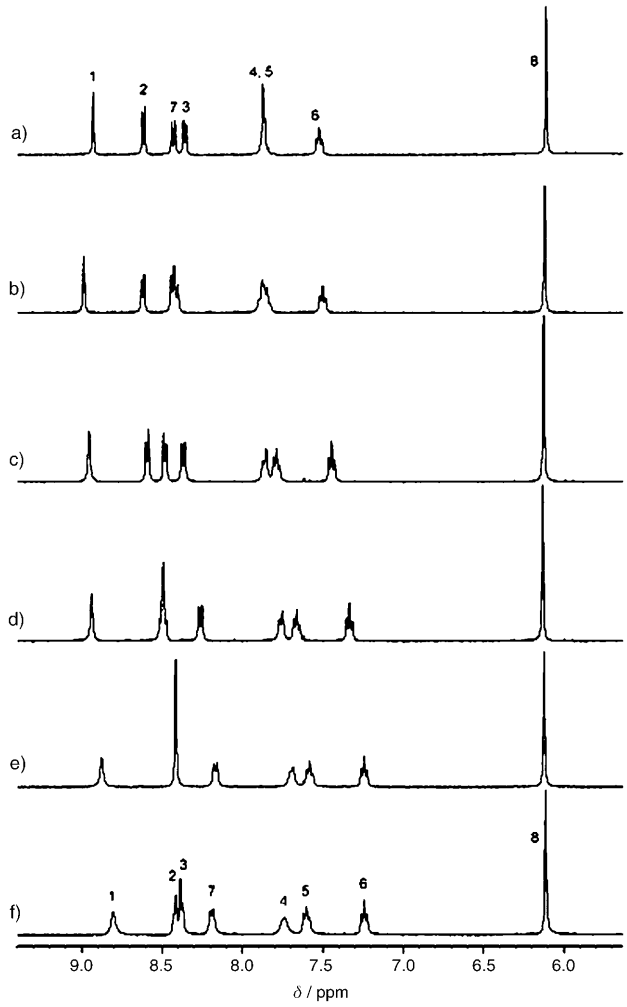

Figure 14. ^{1}H NMR titration of a CD_3CN solution of **3**-$(PF_6)_3$ (1.0×10^{-3} M) with a standard CD_3CN solution of $[Bu_4N]OH$. The spectra were recorded after the addition of 0 (a), 1.0 (b), 1.5 (c), 2.0 (d), 2.5 (e), 3.0 equivalents (f) of hydroxide.

0 to 1 equivalent of added OH^-. After the addition of one equivalent, the shift was inverted, and upfield displacement of the CH(1) signal was observed up to three equivalents. Thus, titration data suggest the existence of three stepwise equilibria [Eqs. (8)–(10)].

$$LH_3^{3+} + OH^- \rightleftharpoons [LH_3\cdots OH]^{2+} \quad (8)$$

$$[LH_3\cdots OH]^{2+} + OH^- \rightleftharpoons LH^+ + 2\,H_2O \quad (9)$$

$$LH^+ + OH^- \rightleftharpoons L + H_2O \quad (10)$$

 © 2005 Wiley-VCH Verlag GmbH & Co. KGaA, Weinheim

Interestingly, in the first step [Eq. (8)], trifurcate receptor $\mathbf{1}^{3+}$ forms a 1:1 complex with hydroxide. Hydrogen-bonded complexes of OH^- are unprecedented. The reported spectroscopic evidence indicates 1:1 stoichiometry of the complex and, in particular, the downfield shift of the CH(1) proton supports the existence of hydrogen-bonding interactions between OH^- and the receptor. In the second step [Eq. (9)], the hydrogen-bound OH^- and added OH^- ions take up two protons from the receptor in an acid/base neutralization process. Then, a third OH^- ion neutralizes the remaining acidic NH group with formation of the zwitterion L [Eq. (10)]. Nonlinear least-squares treatment of the titration data gave the three stepwise equilibrium constants reported in Table 1. The value of $\lg K_1$ is smaller than that observed for Cl^-, which indicates that OH^-, probably owing to its small size, does not interact with all three arms of the receptor. However, the stabilization provided by the triply positively charged cavity allows the formation of a genuine hydrogen-bonded complex and prevents the occurrence of acid/base neutralization (which, on the contrary, was observed with single-arm receptor $\mathbf{2}^{+}$).

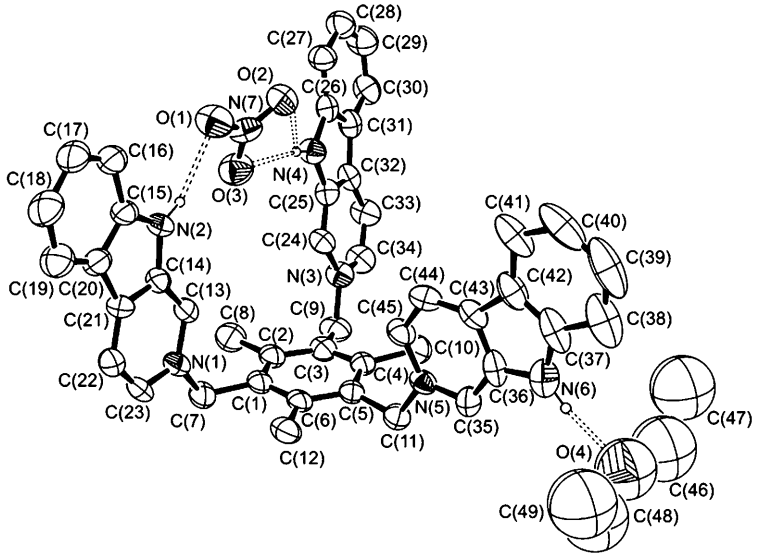

Figure 15. ORTEP view of the $[\mathbf{1}\cdots NO_3]^{2+}\cdot(C_2H_5)O$ complex (non-H atoms are numbered; thermal ellipsoids are drawn at the 30% probability level; only hydrogen atoms bonded to the N(pyrrole) atoms are shown; the two PF_6^- counterions have been omitted for clarity). Dashed lines indicate hydrogen-bonding interactions. Hydrogen-bond lengths [Å] and angles [°]: N(2)···O(1) 2.917(11), H(2N)···O(1) 2.161(8), N(2)–H(2N)···O(1) 146.5(6); N(4)···O(2) 3.059(9), H(4N)···O(2) 2.343(8), N(4)–H(4N)···O(2) 140.9(5); N(4)···O(3) 3.023(9), H(4N)···O(3) 2.195(7), N(4)–H(4N)···O(3) 161.6(5); N(6)···O(4) 2.821(32), H(6N)···O(4) 1.976(29), N(6)–H(6N)···O(4) 167.1(12).

Hydrogen-bonded complexes in the solid state: Attempts were made to obtain crystals suitable for X-ray diffraction studies for all the complexes of $\mathbf{1}^{3+}$ ($=LH_3$) investigated in solution. As a general procedure, diethyl ether vapor was allowed to diffuse into a MeCN solution containing $[LH_3](PF_6)_3$ plus one equivalent or an excess of the envisaged tetrabutylammonium salt. Suitable crystals were obtained only in the case of nitrate. The colorless crystalline product consisted of the receptor–nitrate complex, two PF_6^- counterions, and one molecule of diethyl ether: $[LH_3\cdots NO_3](PF_6)_2\cdot(C_2H_5)_2O$.

Figure 15 shows the ORTEP plot of the complex salt. Of the three pyrrole-containing arms, two are nearly coplanar and point their NH fragments towards the NO_3^- ion, which stays in the middle. The third arm lies in a plane perpendicular to the plane of the other two, but its pyrrole subunit is turned to the outside to allow an N–H···O interaction with the oxygen atom of diethyl ether. Two oxygen atoms of NO_3^- form hydrogen bonds with the N–H group of one arm (O···H 2.19, 2.34 Å), and the third is bound to the N–H group of another arm (O···H 2.16 Å). The hydrogen-bonding interaction between NH and the ethereal oxygen atom appears especially strong, as documented by the rather short O···H distance of 1.98 Å. Availability of the crystal structure is nice, but attributing the same structural arrangement to the $[\mathbf{3}\cdots NO_3]^{2+}$ complex in solution is not straightforward. In particular, one cannot exclude that in solution the receptor is bound to nitrate through all three arms and that in the solid state one arm is diverted from NO_3^- binding due to the presence of diethyl ether as another H-bond acceptor.

No crystals were obtained from a MeCN solution, saturated with diethyl ether, containing equimolar amounts of $\mathbf{3}(PF_6)_3$ and $[Bu_4N]Br$. Instead of disposing of the solution, an excess of $[Bu_4N]OH$ was added, in the hope of inducing crystallization of the fully deprotonated zwitterion L. On further diffusion of diethyl ether, yellow-orange crystals were obtained of a product of formula $[LH_3][LH](PF_6)_3Br\cdot H_2O\cdot 2\,CH_3CN$.

A structural sketch of the complex salt is shown in Figure 16. Two receptor subunits are linked together to form a capsule. The capsule exhibits an overall tetrapositive charge, which is balanced by Br^- and three PF_6^- anions. This indicates that two pyrrole fragments are deprotonated in the capsule. The receptor subunit $L^1H_3^{3+}$ interacts with a Br^- ion, while the other subunit L^2H^+ is doubly deprotonated and includes a water molecule. Deprotonation favors interconnection of the $L^1H_3^{3+}$ and L^2H^+ subunits through a hydrogen-bonding interaction of one negatively charged nitrogen atom of L^2H^+ with an N–H group of the $L^1H_3^{3+}$ moiety. Deprotonation also favors face-to-face π-stacking interactions between the other neutral arm of L^2H^+ (donor) and a positively charged arm of $L^1H_3^{3+}$. In fact, the closest contact (3.36 Å) is observed between C(28) and C(77), the

 © 2005 Wiley-VCH Verlag GmbH & Co. KGaA, Weinheim

Figure 16. A simplified sketch of the $[LH_3]^{3+}[LH]^{+}Br^{-}\cdot H_2O$ complex ($[LH_3]^{3+} = \mathbf{1}^{3+}$; only hydrogen atoms bonded to N atoms and those of the water molecule are shown; three $[PF_6]^{1-}$ ions and two molecules of acetonitrile solvent have been omitted for clarity). Dashed line indicates the N–H···N interaction, which, in addition to face-to-face π-stacking interactions between the aromatic subunits, favors formation of a capsule. Lengths [Å] and angles [°] of the N–H···N interaction: N···N 3.115(14), H···N 2.284(11), N–H···N 162.5(7).

centroid–centroid distance is 3.96 Å, and the dihedral angle between aromatic best planes is 6.2°. These noncovalent interactions between $L^1H_3^{3+}$ and L^2H^{+} are responsible for formation of the capsule.

Figure 17 shows separate ORTEP plots for each moiety of the capsule, to emphasize the interactions of the receptors with the included species. In the $[L^2H\cdots H_2O]^{+}$ complex (left), the water molecule is bound to the three arms 1) as an hydrogen-bond donor to the two negatively charged pyrrole nitrogen atoms, and 2) as an hydrogen-bond acceptor to the NH fragment of the remaining arm. The water oxygen atom is nearly equidistant from the three nitrogen atoms (N(2)–O 3.10(1), N(4)–O 3.12(1), N(6)–O 3.06(2) Å) and is located 0.92(1) Å above the plane of the three N atoms in a slightly distorted trigonal-pyramidal coordination environment. If the behavior in solution reflects the structural aspects of the solid state, the second step of the interaction of $\mathbf{1}^{3+}$ with OH^{-}, which was described by Equation (9), should be more adequately represented by Equation (11).

$$[LH_3\cdots OH]^{2+} + OH^{-} \rightleftharpoons [LH\cdots H_2O]^{+} + H_2O \qquad (11)$$

The $L^1H_3^{3+}$ moiety (Figure 17, right) hosts the bromide ion, which apparently interacts with five protons: three from CH fragments in the *ortho* position of each arm, and two from the NH groups of two pyrrole subunits (Br···H 2.66(1)–2.98(1) Å). The proton of the third pyrrole nitrogen atom stays at a longer distance of 3.21(1) Å, probably because it is also involved in the N–H···N bridge connecting the two receptor subunits and contributes to holding together the capsule. In any case, binding by all three arms with a coordination number of (5+1) would account for the fact that the $[LH_3\cdots Br]^{-}$ complex exhibits an association constant one order of magnitude higher than that of the $[LH_3\cdots NO_3]^{-}$ complex, for which the solid-state structure indicates coordination by only two arms. Such a comparison seems correct since the two anions form complexes of similar stability with single-arm receptor $\mathbf{2}^{+}$.

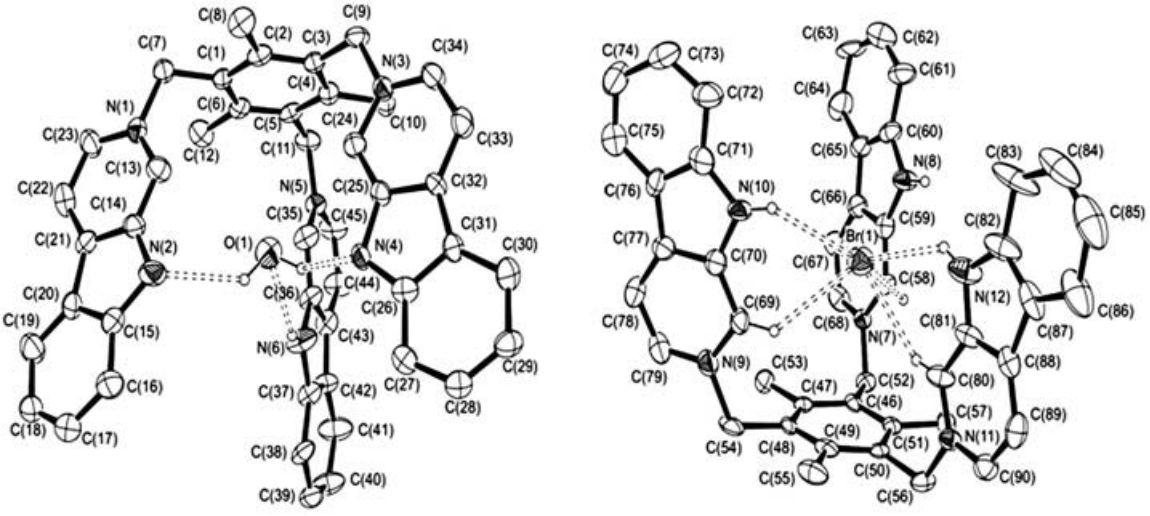

Figure 17. ORTEP plots of the two moieties that form a capsule (non-H atoms are numbered; thermal ellipsoids are drawn at the 30% probability level; only hydrogen atoms bonded to the pyrrole N atoms are shown; the three PF_6^{-} counterions and MeCN molecules of crystallization have been omitted for clarity). Left: the L^2H^{+} moiety, which has two deprotonated pyrrole N–H groups and interacts with an included water molecule through hydrogen bonds (dashed lines); hydrogen-bond lengths [Å] and angles [°]: O(1)···N(2) 3.102(14), H(1W)···N(2) 2.363(87), O(1)–H(1W)···N(2) 137.6(68); O(1)···N(4) 3.117(13), H(2W)···N(4) 2.446(89), O(1)–H(2W)···N(4) 131.4(50); N(6)···O(1) 3.059(16), H(6N)···O(1) 2.352(11), N(6)–H(6N)···O(1) 139.8(75). Right: the $L^1H_3^{3+}$ moiety including a hydrogen-bound bromide ion: dashed lines symbolize the hydrogen bonds between Br^{-} and the closest five protons, whose distances are H(10N) 2.980(13), H(69) 2.757(15), H(12N) 2.778(14), H(80) 2.665(12), H(58) 2.835(14) Å. A sixth proton is more loosely bound: H(8N) 3.206(15) Å.

 © 2005 Wiley-VCH Verlag GmbH & Co. KGaA, Weinheim

Conclusion

The trifurcate trication $\mathbf{1}^{3+}$ is a versatile receptor for anions. It gives very stable 1:1 complexes with halides with a distinct peak selectivity for chloride. Such a high stability must be ascribed to the presence of the positively charged pyridinium groups, which enhance the hydrogen-bond donor tendencies of the CH(1) fragments; as a consequence, the receptor can establish up to six hydrogen bonds with the included anion (three from CH(1) and three from NH fragments). This accounts for the remarkably higher affinity of $\mathbf{1}^{3+}$ towards chloride with respect to fluoride. In fact, F^- is too small to attain the full coordination experienced by the larger Cl^- ion and is forced to interact, albeit strongly, with a single arm of the trifurcate receptor. Thus, interestingly, $\mathbf{1}^{3+}$ selectively discriminates chloride over fluoride when anions are present in substoichiometric amount with respect to the receptor. Moreover, the more basic anions F^- and CH_3COO^-, when present in excess, induce deprotonation of the pyrrole NH groups, an event which is signaled by development of an intense absorption band in the visible region and by the upfield shift of receptor protons, including CH(1). The occurrence of the neutralization process can hardly be missed, as it is visually perceived through the appearance of a bright yellow color. However, the most surprising interaction established by $\mathbf{1}^{3+}$ is that with the OH^- ion. In particular, hydroxide forms a novel and authentic 1:1 complex with $\mathbf{1}^{3+}$. We do not know the structural details of the $[LH_3\cdots OH]^{2+}$ complex: certainly, the H-bound OH^- ion is included within the cavity, the triply positively charged internal environment of which must play a determining role. In fact, in the presence of the "open" NH site of the reference receptor $\mathbf{2}^{+}$, OH^- displays its normal and expected behavior as a strong base by abstracting a proton to give neutralization. Thus, occasionally, with complicity of the trifurcate receptor $\mathbf{1}^{3+}$, the OH^- ion leaves the classic domain of Brønsted acid–base reactions and visits, perhaps for the first time, the enchanted realm of supramolecular chemistry.

Experimental Section

General procedures and materials: All reagents for syntheses were purchased from Aldrich/Fluka and used without further purification. UV/Vis spectra were recorded on a Varian CARY 100 spectrophotometer with a quartz cuvette (path length: 1 or 0.1 cm) and on a Hewlett Packard 8452 A spectrophotometer with a quartz cuvette (path length: 10 cm). The cell holder was thermostatically maintained at 25.0 °C by circulating water. ^{1}H NMR spectra were obtained on a Bruker AVANCE 400 spectrometer (400 MHz) operating at 9.37 T. Spectrophotometric titrations were performed on $(1–7)\times10^{-4}$ M solutions of $\mathbf{2}^{+}$ in MeCN (polarographic grade); for $\mathbf{1}^{3+}$, a wider range of concentrations was used, generally from 10^{-4} to 10^{-6} M in MeCN. Typically, aliquots of a fresh standard solution of an alkylammonium salt of the envisaged anion (CH_3COO^-, $C_6H_5COO^-$, $H_2PO_4^-$, NO_2^-, HSO_4^-, NO_3^-, F^-, Cl^-) were added, and the UV/Vis spectra of the samples recorded. Tetrabutylammonium salts were used for all anions, but for chloride, for which the benzyltributylammonium ion was used, which gives a nonhygroscopic salt). All spectrophotometric titration curves were fitted with the HYPERQUAD program.[21] Care was taken that in each titration the p parameter (p = [concentration of complex]/[maximum possible concentration of complex]) was less than than 0.8, a condition required for the safe determination of a reliable equilibrium constant.[22] ^{1}H NMR titrations were carried out on CD_3CN solutions at a receptor of 10^{-3}–10^{-2} M. In general, the equilibrium constant could not be calculated from ^{1}H NMR titration experiments, because at the employed concentrations steep titration profiles were obtained with p values higher than 0.8, which prevented reliable evaluation of $\lg K$.

Synthesis and characterization: The synthesis of 9*H*-β-carbolin-2-ium hexafluorophosphate (**4**-PF_6) has been already described.[16]

1,3,5-tris(9*H*-β-carbolinium-*N*-methyl)-2,4,6-trimethylbenzene hexafluorophosphate (3-(PF_6)$_3$): β-Carboline (0.26 g, 1.53 mmol) was dissolved in $CHCl_3$ (80 mL). 1,3,5-Tris(bromomethyl)-2,4,6-trimethylbenzene (0.15 g, 0.38 mmol) in $CHCl_3$ (15 mL) was added and the obtained solution was refluxed for 24 h, during which a yellow precipitate formed. The solid was filtered off, dissolved in H_2O/MeOH (50 mL, 4/1), and treated with a saturated aqueous solution of NH_4PF_6. The white hygroscopic precipitate of **3**-(PF_6)$_3$ was recovered by filtration and washed with several portions of diethyl ether (yield: 0.33 g, 80 %). $C_{45}H_{39}N_6P_6F_{18}$ (1098.5 g mol^{-1}). ^{1}H NMR (400 MHz, CD_3CN, 25 °C, TMS): δ = 8.9 (s, 1H; CH), 8.6 (d, 1H; CH), 8.4 (d, 1H; CH), 8.4(d, 1H; CH), 7.8 (d, 2H; 2CH), 7.5 (m, 1H; CH), 6.1 (s, 2H; CH_2), 2.3 ppm (s, 3H; CH_3).

X-ray crystallographic studies: Several attempts to obtain suitable materials were carried out, but in general single crystal were too small for

Table 2. Crystal data for the complex salts.

	$[LH_3\cdots NO_3][PF_6]_2\cdot(C_2H_5)_2O$	$[LH_3][LH](PF_6)_3Br\cdot H_2O\cdot 2CH_3CN$
formula	$C_{49}H_{49}F_{12}N_7O_4P_2$	$C_{94}H_{84}BrF_{18}N_{14}OP_3$
M_r	1089.89	1940.56
color	colorless	deep yellow
dimensions [mm]	$0.20\times0.10\times0.06$	$0.13\times0.12\times0.02$
crystal system	triclinic	triclinic
space group	$P\bar{1}$ (no. 2)	$P\bar{1}$ (no. 2)
a [Å]	11.2743(26)	13.0056(8)
b [Å]	14.7569(33)	14.8514(9)
c [Å]	15.9934 (36)	22.8499(14)
α [°]	104.187(4)	100.043(2)
β [°]	106.520(4)	96.897(2)
γ [°]	93.215(4)	93.640(2)
V [Å^3]	2450.4(10)	4298.3(5)
Z	2	2
ρ_{calcd} [g cm^{-3}]	1.477	1.499
$\mu(Mo_{K\alpha})$ [mm^{-1}]	0.188	0.633
scan type	ω scans	ω scans
θ range [°]	2–21	2–22
measured reflections	11621	23674
unique reflections	4876	10524
R_{int}	0.0504	0.0475
strong data [$I_o > 2\sigma(I_o)$]	3035	7130
$R1$, $wR2$ (strong data)	0.1106, 0.3072	0.1299, 0.3383
$R1$, $wR2$ (all data)	0.1529, 0.3423	0.1661, 0.3657
GOF	1.212	1.061
refined parameters	645	1194
max/min residuals [e Å^{-3}]	0.54/−0.42	1.11/−1.28

© 2005 Wiley-VCH Verlag GmbH & Co. KGaA, Weinheim

crystallographic study. The crystals selected for data collection also showed a low diffraction power and hence rather high final agreement indexes. However, the crystallographic details are unambiguous and the interpretation of structural features feasible. Diffraction data were collected at room temperature on a Bruker-Axs Smart-Apex CCD-based diffractometer with graphite-monochromatized $Mo_{K\alpha}$ radiation ($\lambda =$ 0.71073 Å). Crystal data for $[LH_3{\cdots}NO_3][PF_6]_2{\cdot}(C_2H_5)_2O$ and $[LH_3][LH](PF_6)_3Br{\cdot}H_2O{\cdot}2\,CH_3CN$ are reported in Table 2

Data reductions (including intensity integration, and background, Lorentzian, and polarization corrections) were performed with the SAINT software (Bruker-Axs, Inc.) Absorption effects were analytically evaluated by the SADABS software,[23] and absorption correction was applied to the data (min./max. transmission factors were 0.75/0.98 and 0.85/0.98). Crystal structures were solved by direct methods (SIR97)[24] and refined by full-matrix least-square procedures on F^2 for all reflections (SHELXL97).[25] Calculations were performed with the WinGX package.[26] Anisotropic displacement parameters were refined for all non-hydrogen atoms, excluding diethyl ether (refined with isotropic atom-displacement factor). Hydrogen atoms were placed at calculated positions with the appropriate AFIX instructions and refined by using a riding model.

CCDC-266162 and CCDC-266163 contain the supplementary crystallographic data for this paper. These data can be obtained free of charge from the Cambridge Crystallographic Data Centre via www.ccdc.cam.ac.uk/data_request/cif.

Acknowledgements

We thank Dr. Laura Linati (Centro Grandi Strumenti, Università di Pavia) for the NMR characterization of the samples and Dr. Enrico Monzani (Dipartimento di Chimica Generale, Università di Pavia) for assistance in the NMR titrations and helpful discussion. The financial support of the Italian Ministry of University and Research (PRIN - Dispositivi Supramolecolari; FIRB - Project RBNE019H9K) is gratefully acknowledged.

[1] P. D. Beer, P. A. Gale, *Angew. Chem.* **2001**, *113*, 502–532; *Angew. Chem. Int. Ed.* **2001**, *40*, 486–516
[2] Special issue: *Coord. Chem. Rev.* **2003**, *240*, 1–226.
[3] T. Clifford, A. Danby, J. M. Llinares, S. Mason, N. W. Alcock, D. Powell, J. A. Aguilar, E. Garcia-Espana, K. Bowman-James, *Inorg. Chem.* **2001**, *40*, 4710–4720.
[4] F. P. Schmidtchen, *Angew. Chem.* **1977**, *89*, 751–752; *Angew. Chem. Int. Ed. Engl.* **1977**, *16*, 720–721.
[5] M. Berger, F. P. Schmidtchen, *J. Am. Chem. Soc.* **1996**, *118*, 8947–8948.
[6] V. Amendola, L. Fabbrizzi, E. Monzani, *Chem. Eur. J.* **2004**, *10*, 76–82.
[7] S. Yun, H. Ihm, H. G. Kim, C.-W. Lee, B. Indrajit, K. S. Oh, Y. J. Gong, J. W. Lee, J. Yoon, H. C. Lee, K. S. Kim, *J. Org. Chem.* **2003**, *68*, 2467–2470.
[8] M. Boiocchi, M. Bonizzoni, L. Fabbrizzi, G. Piovani, A. Taglietti, *Angew. Chem.* **2004**, *116*, 3935–3940; *Angew. Chem. Int. Ed.* **2004**, *43*, 3847–3852.
[9] K. Kavallieratos, C. M. Bertao, R. H. Crabtree, *J. Org. Chem.* **1999**, *64*, 1675–1683.
[10] S.-I. Kondo, T. Suzuki, Y. Yano, *Tetrahedron Lett.* **2002**, *43*, 7059–7061.
[11] P. J. Smith, M. V. Reddington, C. S. Wilcox, *Tetrahedron Lett.* **1992**, *33*, 6085–6088.
[12] J. L. Sessler, M. J. Cyr, V. Lynch, E. McGhee, J. A. Ibers, *J. Am. Chem. Soc.* **1990**, *112*, 2810–2813.
[13] S. O. Kang, J. M. Llinares, D. Powell, D. van der Velde, K. Bowman-James, *J. Am. Chem. Soc.* **2003**, *125*, 10152–10153.
[14] S. Valiyaveetil, J. F. J. Engbersen, W. Verboom, D. N. Reinhoudt, *Angew. Chem.* **1993**, *105*, 942–944; *Angew. Chem. Int. Ed. Engl.* **1993**, *32*, 900–901.
[15] A. Metzger, E. V. Anslyn, *Angew. Chem.* **1998**, *110*, 682–684; *Angew. Chem. Int. Ed.* **1998**, *37*, 649–652.
[16] V. Amendola, M. Boiocchi, L. Fabbrizzi, A. Palchetti, *Chem. Eur. J.* **2005**, *11*, 120–127.
[17] K. J. Wallace, W. J. Belcher, D. R. Turner, K. F. Syed, J. W. Steed, *J. Am. Chem. Soc.* **2003**, *125*, 9699–9715.
[18] S. Gronert, *J. Am. Chem. Soc.* **1993**, *115*, 10258–10266.
[19] S. Camiolo, P. A. Gale, M. B. Hursthouse, M. E. Light, A. I. Shi, *Chem. Commun.* **2002**, 758–759.
[20] T. Steiner, *Angew. Chem.* **2002**, *114*, 50–80; *Angew. Chem. Int. Ed.* **2002**, *41*, 48–76.
[21] P. Gans, A. Sabatini, A. Vacca, *Talanta* **1996**, *43*, 1739–1753.
[22] C. S. Wilcox in *Frontiers of Supramolecular Chemistry and Photochemistry* (Eds.: H.-J. Schneider, H. Dürr), Wiley-VCH, Weinheim, **1991**, pp. 123–143.
[23] G. M. Sheldrick, SADABS, Siemens Area Detector Absorption Correction Program, University of Göttingen: Göttingen, Germany, **1996**.
[24] A. Altomare, M. C. Burla, M. Camalli, G. L. Cascarano, C. Giacovazzo, A. Guagliardi, A. G. G. Moliterni, G. Polidori, R. Spagna, *J. Appl. Crystallogr.* **1999**, *32*, 115–119.
[25] G. M. Sheldrick, SHELX97, Programs for Crystal Structure Analysis, University of Göttingen, Göttingen, Germany, **1997**.
[26] L. J. Faia, *J. Appl. Crystallogr.* **1999**, *32*, 837–838.

Received: March 28, 2005
Published online: July 15, 2005

 © 2005 Wiley-VCH Verlag GmbH & Co. KGaA, Weinheim